

## Size and charge effects on the deposition of Na on Ar

P. M. Dinh<sup>1</sup>, F. Fehrer<sup>2</sup>, P.-G. Reinhard<sup>2</sup>, and E. Suraud<sup>1</sup>

<sup>1</sup>*Laboratoire de Physique Théorique, UMR 5152, Université Paul Sabatier, 118 route de Narbonne, F-31062 Toulouse Cedex, France*

<sup>2</sup>*Institut für Theoretische Physik, Universität Erlangen Stadtstr. 7, D-91058 Erlangen, Germany*

We discuss the dynamical deposition of the Na atom, the Na<sup>+</sup> ion and the Na-6 cluster on finite Ar clusters mocking up an infinite Ar surface. We analyze this scenario as a function of projectile initial kinetic energy and of the size of the target cluster.

### 1. Introduction

Clusters on surfaces have motivated many studies over the past decades and still remain a topic of great interest,<sup>1</sup> especially in relation to the synthesis of nanostructured surfaces.<sup>2-5</sup> Indeed, it turns out that it is possible to make a direct deposition of size selected clusters on a substrate.<sup>6,7</sup> The deposition process may lead to a significant modification of the cluster, in terms of its electronic structure and ionic geometry. This is a consequence of the impact of the interface energy, the electronic band structure of the substrate, and the surface corrugation. These questions have already been widely investigated in great detail, especially from the structural point of view and both from the experimental<sup>8-10</sup> and theoretical<sup>11-18</sup> sides. The situation is somewhat different concerning the deposition process itself. Its theoretical description remains mostly limited to molecular dynamics (MD) approaches, which implies that a proper description of electronic degrees of freedom is missing. The reason for this defect is simple. The presence of a substrate makes the experimental handling of clusters easier but strongly complicates the theoretical description because of the huge number of degrees of freedom of the surface. The MD then provides the cheapest way to access, at least in a gross way, the dynamics of the substrate. It is nevertheless crucial to try to account for the surface's electronic degrees of freedom, for example when non adiabatic processes are involved.

As a first step in the direction of a fully microscopic dynamical approach, one may consider relatively simple cluster/substrate combinations. This is for example the case of the deposit of a metal cluster on an insulator surface. The surface can then be included at a lower level of description, which simplifies the handling, as was, e.g., explored for the case of Na clusters on NaCl in.<sup>18,19</sup> Cluster electrons were there described by means of Density Functional Theory and the coupling to

the surface was achieved *via* an effective interface potential, itself tuned to *ab-initio* calculations.<sup>14</sup> Such an approach implies a total freezing of the surface itself, which sets severe limitations on its applicability. A somewhat better description of surface degrees of freedom in a still limited/simplified way can be achieved by considering again a rather inert substrate, but allowing for a minimum of dynamical response of the substrate. Such a model was recently proposed for describing sodium clusters embedded in rare gases.<sup>20–22</sup> The method used was "hierarchical", which is justified by the moderate interactions between cluster and surface. The interface can then be treated at a simpler level than the cluster's degrees of freedom (microscopic treatment of cluster and classical treatment of environment with explicit account of dynamical polarizability effects), in the spirit of the coupled quantum-mechanical with molecular-mechanical method (QM/MM) often used in bio-chemistry.<sup>23–25</sup>

Such hierarchical methods, although much simpler than a fully microscopic approach, require sophisticated modeling and are thus restricted to finite systems. Nonetheless, the calculations in<sup>21,22</sup> were carried forth to a sufficiently large range of sizes to see the appearance of generic behaviors on the way towards the bulk. In the complementing case of deposit on a surface, we also consider finite substrates, as model cases for a surface. This is an acceptable compromise once the impact of the finiteness of the substrate has been properly analyzed. For a first exploration, we went one step further and restricted the present analysis to the even simpler case of the deposition of a single Na atom on a finite Ar cluster, adding one test case in which we shall explore the case of a finite Na cluster.

The goal of this paper is thus mostly the study of the dynamics of deposition of a sodium atom (projectile) on Ar clusters of various sizes  $\text{Ar}_N$  (target,  $N = 43, 86$ ). We shall analyze the behaviors of both the atom and the cluster, especially as a function of deposit velocity and also consider size and charge effects (deposit of a  $\text{Na}_6$  cluster and a  $\text{Na}^+$  ion instead of a Na atom). The paper is organized as follows. Section 2 gives a short presentation of the model used. A few more details on the model can be found in the appendix, where basic formulae and parameters are recalled. The following sections successively address the dependence on substrate size and on projectile velocity. We finally discuss the example of a true cluster deposit and of charge effects.

## 2. Model

The model was presented in detail in<sup>26</sup> and we provide the basic formulae in the appendix. We recall briefly the basic ingredients. The Na cluster is described in terms of time-dependent local-density approximation for the electrons coupled to molecular dynamics for the ions (TDLDA-MD), a scheme which has been extensively validated for linear and non-linear dynamics in free metal clusters.<sup>27,28</sup> The electron-ion interaction is treated by means of a soft, local pseudo-potentials.<sup>29</sup> Each Ar atom is described by two classical degrees-of-freedom: its center-of-mass and its electrical dipole moment. The explicit account of Ar dipoles allows to treat

the polarizability of the atoms dynamically, with help of polarization potentials.<sup>30</sup> Atom-atom interactions are described by a standard Lennard-Jones potential. For the Ar-Na<sup>+</sup> interaction we employ effective potentials from the literature.<sup>31</sup> The electron-Ar core repulsion is modeled in the form proposed by,<sup>32</sup> with a slight final readjustment of the parameters to the NaAr molecule as benchmark (bond length, binding energy and optical excitation). A Van der Waals interaction is also added and computed *via* the variance of dipole operators.<sup>20,26,32</sup>

Na@Ar<sub>86</sub> ○

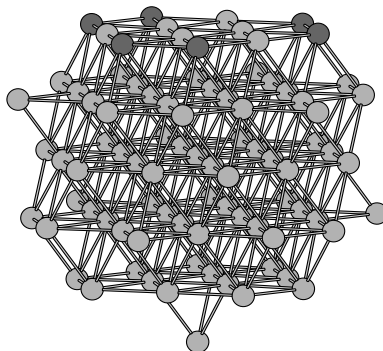


Fig. 1. Atomic configuration of Ar<sub>86</sub> with respect to the single Na (white ball). Six Ar atoms are emphasized by dark gray balls for the discussion on Na<sup>+</sup> deposition in Ar<sub>86</sub> (see text).

As explained in the appendix, the starting quantity is the total energy, constructed from the various pieces discussed above. The corresponding equations of motion can then be derived by standard variation, which leads to the time-dependent Kohn-Sham equations for the cluster electrons. One furthermore obtains Hamiltonian equations of motion for the classical degrees of freedom (Na<sup>+</sup> ions as well as Ar atom positions and dipoles). The initial condition is provided by the corresponding stationary solutions.

The definition of the Ar-Na configuration requires some specific handling. Indeed the Na atom can be initially placed above either an Ar atom or an interstitial site of the surface layer. In the case of Ar<sub>43</sub> (see Figure 2), the first option has been chosen, and for Ar<sub>86</sub>, the second initial configuration has been used, see Figure 1. The Ar<sub>86</sub> is obtained from the stable free Ar<sub>87</sub> cluster where an outer Ar atom has been removed. The resulting Ar<sub>86</sub> is then rotated in order to present a flat surface to the impinging Na atom, this way simulating the flat interface provided by an infinite surface. The starting configuration for the deposit of Na<sub>6</sub> on Ar<sub>43</sub> is similar

to that of the single Na atom. This means the top Na ion (the  $\text{Na}_6$  is composed of a ring of 5 ions and an outer ion) is placed above an Ar atom.

The numerical solution proceeds with standard methods as detailed in.<sup>28</sup> The Kohn-Sham equations for the cluster electrons are solved using real space grid techniques. The time propagation proceeds using a time-splitting method. The stationary solution is attained by accelerated gradient iterations. We furthermore employ the cylindrically-averaged pseudo-potential scheme (CAPS) as introduced in,<sup>33,34</sup> an approximation justified for the chosen test cases. In the following, the symmetry axis is denoted by the  $z$  axis. It should nevertheless be noted that the dynamics of the  $\text{Na}^+$  ions as well as that of the Ar atoms are treated in full 3D.

### 3. Dynamical deposition of Na on finite Ar clusters

#### 3.1. *An example*

We first consider, as an example, the case of the deposition of a Na atom on an  $\text{Ar}_{43}$  cluster. This is illustrated in Figure 2 where a few snapshots of the deposition process are presented. In that test case, the Ar cluster presents to the Na atom a rather small surface area of only 5 atoms and the the Na atom is initially positioned above an Ar atom (which shows strong core repulsion). These two features differ as compared to the case of  $\text{Ar}_{86}$  illustrated in Figure 1 and discussed later on in Section 3.3. They should *a priori* make an attachment of the Na sodium more difficult here. Still, the calculation shows that a faint binding takes place in this case within typically 3 ps. The Na atom loosely attaches to the Ar cluster surface, since it keeps on bouncing over 7 ps with a decreasing amplitude and around an average position of about  $8 a_0$ , even a bit closer than the NaAr dimer bond length of  $9.5 a_0$ . Mind that the initial Na kinetic energy  $E_0$  was 13.6 meV, in between the 5 meV binding energy of the NaAr dimer and the 50 meV of the bonding in Ar bulk. Thus there is no surprise to observe the creation of a transient NaAr bond and a very slight rearrangement of the Ar cluster, which takes place over a time scale of order of 5 ps. Actually, the Na atom is accelerated during its fall and gets, before the hit, a kinetic energy almost three times higher than  $E_0$  (this depends on its initial separation with the Ar first layer). Then after the hit, the extra kinetic energy is absorbed by the Ar cluster both at the side of kinetic energy (about 15 meV) and in terms of potential energy in its structure rearrangement. The residual kinetic energy of Ar atoms as well as the potential energy consumed in the Ar cluster rearrangement strongly depend on the available energy and the number of degrees of freedom. It is thus interesting to study the effect of variations of both these parameters.

#### 3.2. *Dependence on kinetic energy*

We first consider the influence of the initial kinetic energy of the Na projectile. The results are displayed in Figure 3 for the deposition of a Na atom on  $\text{Ar}_{86}$  at

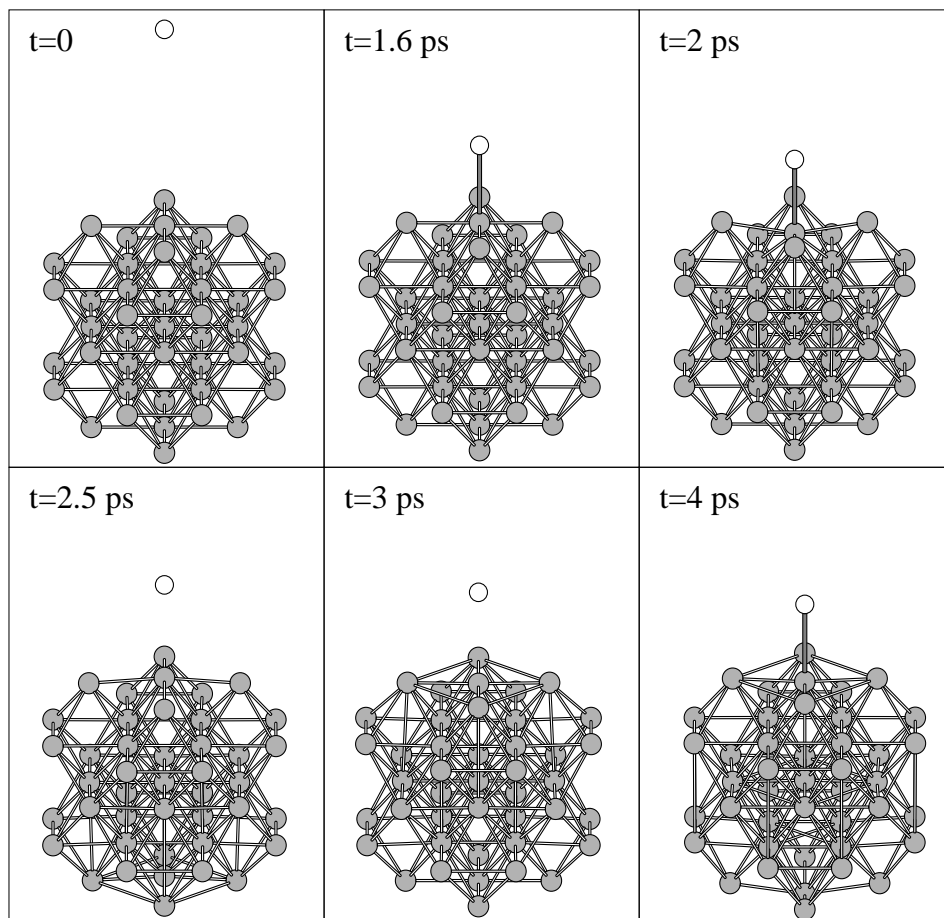


Fig. 2. Example of dynamical deposition of a Na atom on an  $\text{Ar}_{43}$  cluster, with initial kinetic energy  $E_0 = 13.6$  meV.

various energies ( $E_0 = 13.6$  to  $870$  meV). It should first be noted that, whatever the initial kinetic energy no electronic emission is observed. We shall thus restrict the discussion to ionic and atomic degrees of freedom. In the case of the two lowest impact energies, one observes some bounces, and finally a binding of the Na to the surface at a typical distance of about  $8 - 10 a_0$  from the first layer. However for higher  $E_0$ , the Na is reflected by the Ar cluster, and no attachment of the Na is observed, although the Na is initially located above an interstitial position. This result can be confirmed by computing the Born-Oppenheimer surface of Na on an infinite Ar surface. The ground state surface exhibits a faint minimum around  $7 a_0$  above the Ar surface, which is fully compatible with our dynamical analysis on the finite  $\text{Ar}_{86}$  cluster. Closer to the Ar surface, the Born-Oppenheimer surface exhibits a strong repulsion reflecting the core repulsion between Na and Ar. When the impact

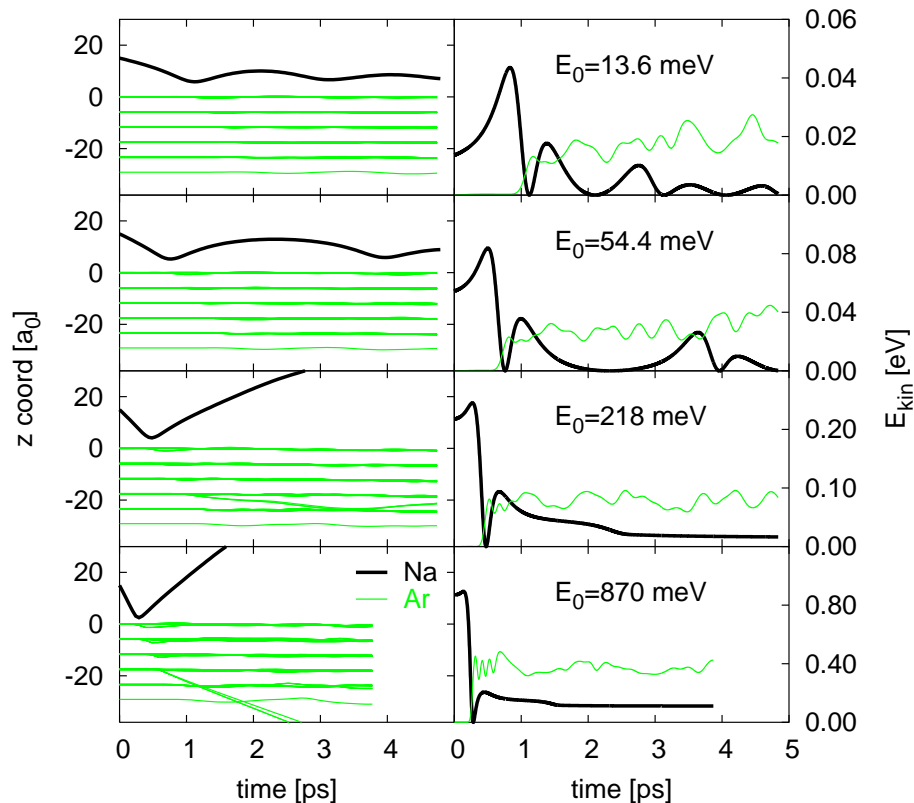


Fig. 3. Dynamical deposition of Na (thick lines) on  $\text{Ar}_{86}$  for four different initial kinetic energies. The  $z$ -coordinates (left) and the kinetic energies (right) are presented as a function of time.

kinetic energy becomes too large the Na atom thus "misses" the faint minimum and directly explores the strongly repulsive part of the potential. The Na atom is then reflected by the cluster as observed in Figure 3. The energy threshold for neutral Na sticking seems to lie between 0.05 and 0.2 eV. Note that in this range of kinetic energies, the Ar cluster is not affected very much. This is particularly visible on the time dependence of its kinetic energy, which exhibits a rather smooth energy transfer from the Na to the Ar cluster. We also observe the propagation of a soft shock wave in the substrate. This participates to the slight heating of the Ar cluster (to a few tens of K), except for the highest energy where some deep Ar atoms are emitted because of the stronger wave propagating through the layers.

### 3.3. Dependence on Ar cluster size

We now consider the influence of the number of degrees of freedom on the capacity to dissipate the available energy. In practice, this amounts to test the influence of the Ar cluster size for constant initial kinetic energy of the Na atom. The comparison

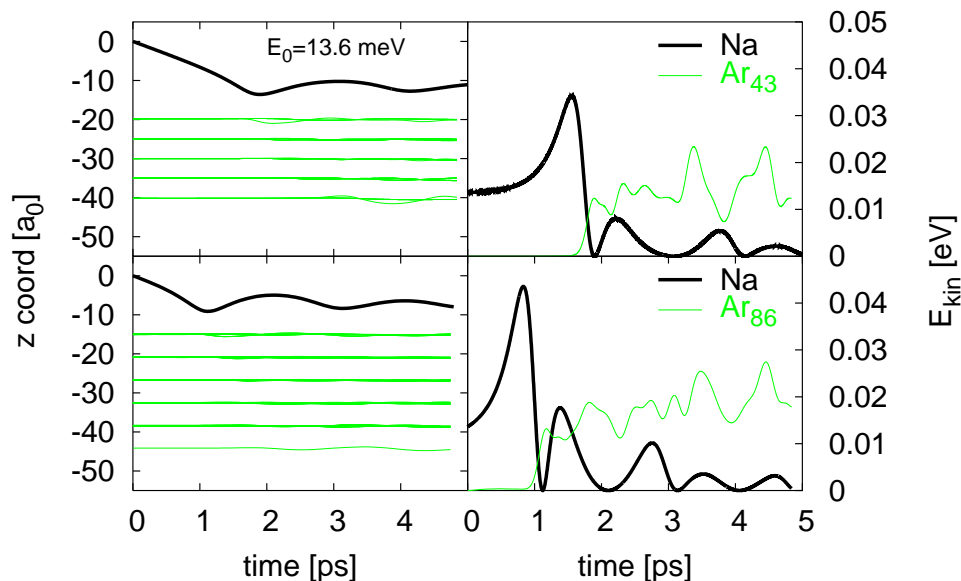


Fig. 4. Deposit of a single Na atom ( $E_0 = 13.6$ ) on  $Ar_N$  systems of various sizes ( $N = 43$  and  $86$ ). Are presented as a function of time, the  $z$  coordinates (left) and the kinetic energies (right) of the Na atom (thick lines) and the Ar cluster (thin curves).

is presented in Figure 4 where we plot Na and Ar positions and kinetic energies as a function of time during the deposition process of a Na atom (with initial kinetic energy  $E_0$  of 13.6 meV) on  $Ar_{43}$  and  $Ar_{86}$ . As already mentioned, two main differences between both cases are to be noted. First the Na atom is initially above an Ar atom of the  $Ar_{43}$ , at a distance of  $20 a_0$ . In the case of  $Ar_{86}$ , the Na atom is above an interstitial site and starts at a smaller distance from the Ar first layer, namely  $15 a_0$ . Due to their different sizes, the effective Ar surface exhibits only 5 atoms in the case of  $Ar_{43}$  but 12 Ar atoms for  $Ar_{86}$ .

Similar oscillating patterns are observed in both cases. 2 ps after the impact, almost all kinetic energy of the Na atom is transferred to the Ar cluster, while the Ar kinetic energy seems to reach an equilibrium and oscillates around a mean value slightly higher than the initial kinetic energy  $E_0$ . Mind that the transferred energy is distributed equally over all Ar atoms. This means that, as expected, the larger the target cluster size (thus the more available degrees of freedom), the smaller the relative energy shared per Ar atom, and so the more moderate the perturbation at their side. Note, furthermore, that more Na kinetic energy is available at the time of impact (maximum of Na kinetic energy in the right panels) for the case of  $Ar_{86}$ . This means that the Na atom is accelerated faster in that case as compared with  $Ar_{43}$ . The reason is that the larger cluster and its larger surface area provide more attraction from polarization potentials. Nonetheless, in both cases, the Na atom

loosely binds to the surface, at about the same distance of about  $8 a_0$ .

#### 4. Example of a finite cluster deposit

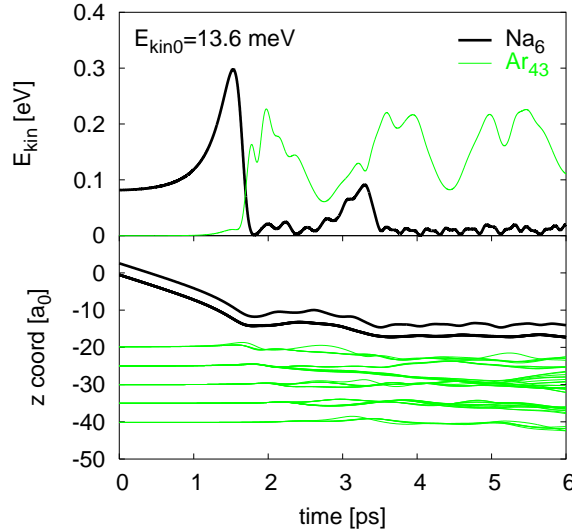


Fig. 5. Example of deposit of a finite  $\text{Na}_6$  cluster on  $\text{Ar}_{43}$ .

In order to complement the analysis in terms of Ar cluster size, it is also interesting to consider the case of the deposition of a full Na cluster, instead of a single atom. This again enhances the number of degrees of freedom. We shall consider comparable impact kinetic energy per Na atom. In Figure 5 we consider an example of a deposition of a finite Na cluster ( $\text{Na}_6$ ) on  $\text{Ar}_{43}$ . The initial kinetic energy of the cluster is  $E_{\text{kin}0} = 13.6$  meV per Na atom. As in the case of a single Na atom (Figure 2) the pinning process proceeds stepwise with a slight bounce before the metal cluster finally attaches to the rare gas cluster. At variance with the case of a single atom, though, one can furthermore analyze the evolution of the shape of the deposited Na cluster. The considered  $\text{Na}_6$  cluster is primarily strongly oblate, consisting of a pentagon of 5 Na atoms topped by one central atom. One can see that during the deposition process, the cluster shape is little affected. This might have been expected in view of the ideal "flat" shape of the  $\text{Na}_6$  cluster which already presents a large contact area to the Ar surface. But we also found for other, and less favorable, geometries (e.g. the nearly spherical  $\text{Na}_8$  cluster) that the cluster shape remains basically intact during deposition. The details of this scenario of course depend on the size of the Ar cluster target and on the initial kinetic energy of the impinging Na cluster, but qualitatively the example displayed in Figure 5 turns out to be quite typical. These results will be presented elsewhere.<sup>38</sup>



## 5. Charge effects

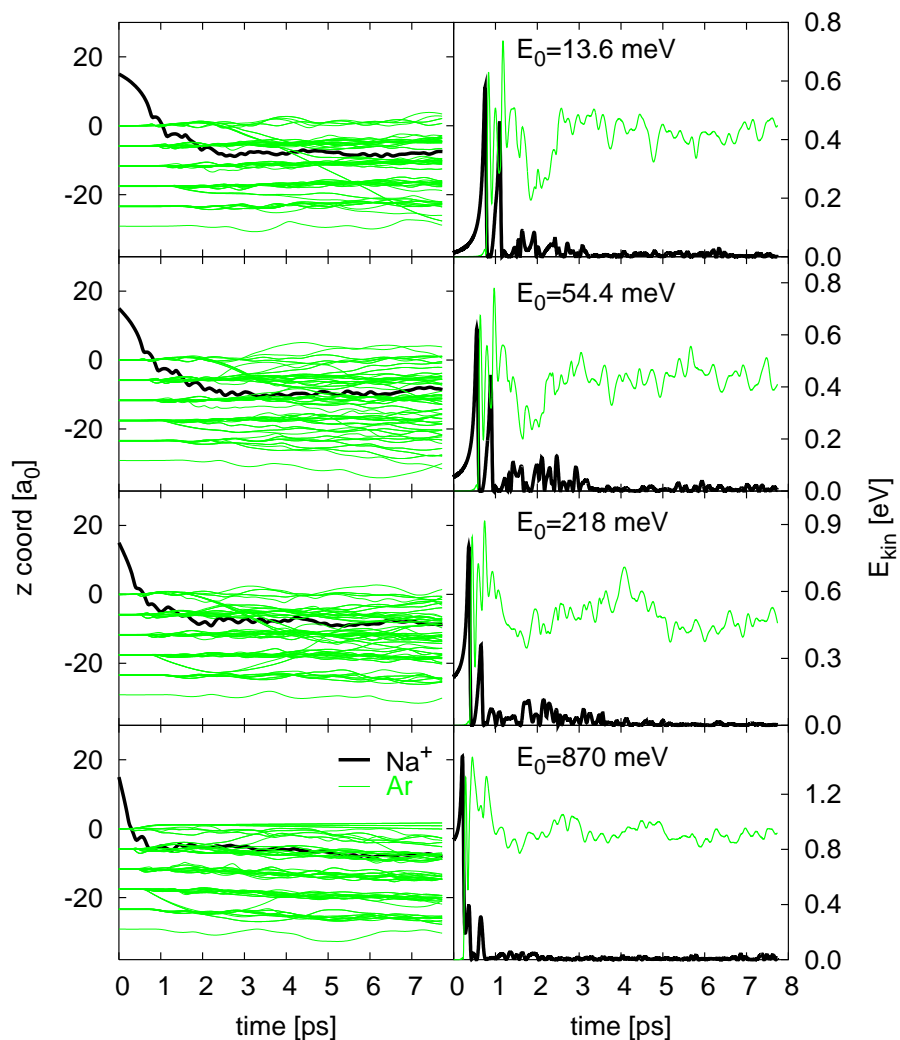


Fig. 6. Same as in Figure 3, in the case of  $\text{Na}^+$  on  $\text{Ar}_{86}$ .

As a final point, we want now to analyze the influence of charge on the deposition process. We come back to the simple case of a single Na atom and consider the deposition of the corresponding  $\text{Na}^+$  ion on  $\text{Ar}_{86}$ , at various initial kinetic energies. Born Oppenheimer calculations of  $\text{Na}^+$  in contact to an Ar surface show that the attachment is much stronger (and closer to the surface) than in the case of the neutral species. This can be easily understood by remembering the key role played by

the attractive Ar polarization potentials. The finite charge of the  $\text{Na}^+$  ion strongly polarizes the surface and thus enhances the binding as compared to the neutral case. Of course short range repulsion remains present but will take the lead only on shorter distances. The attachment is thus expected to be stronger and closer to the surface.

Figure 6 confirms the expectation. The  $\text{Na}^+$  ion is practically swallowed by the Ar cluster and the Ar cluster itself undergoes stronger rearrangements. For the smallest  $E_0$  presented in the top panels of Figure 6, two of the six surface atoms are finally ejected from the Ar cluster (they are visible by the light lines going straight through Ar layers in the  $z$ -coordinate panel and having reached the lower end at 7 ps). The four other Ar atoms of the (strongly perturbed) surface remain bound to the whole cluster and participate to its strong rearrangement. In the case of intermediate  $E_0$ , the six Ar atoms are lifted from the first layer but still stick to the edges of the Ar cluster. The fact that the  $\text{Na}^+$  goes deeper for  $E_0 = 54.4$  meV seems to be due to the final ejection of an Ar atom. In the latter three cases, these six atoms get about 10% of the total Ar kinetic energy. Finally, for the highest  $E_0$ , the first layer just explodes after the impact. The six outmost Ar atoms absorb up to 50% of the vertical shock in term of kinetic energy transfer, and then follow a radial motion in an horizontal plane (see the thin horizontal lines around  $z = 0$  in the bottom left panel of Fig.6). In all cases, the removal of the six atoms from the first Ar layer, either outside or at the edges of the Ar cluster, allows some Ar atoms deeper inside the substrate to move upwards, thus leaving a large vacancy, so that the  $\text{Na}^+$  can penetrate even under the second layer. These results suggest that the number of layers under the Ar surface probably does not play an important role in the  $\text{Na}^+$  inclusion. More important is the surface's mobility for rearrangements.

## 6. Conclusion

In this paper, we have presented results on the deposition of a Na atom, a  $\text{Na}^+$  ion, and a  $\text{Na}_6$  cluster on a dynamically polarizable Ar substrate represented by finite Ar clusters of various sizes. We have used time-dependent density-functional theory for the Na electrons coupled to molecular dynamics for the treatment of Na ions and Ar atoms. We have presented systematic results as a function of Ar cluster size and kinetic energy of the impinging Na atom. We have found that the neutral Na is not likely to penetrate into the Ar matrix and sticks to the Ar surface for initial kinetic energy lower than  $\sim 0.2$  meV while being reflected for larger impact kinetic energies. In case of the positively charged  $\text{Na}^+$ , inclusion is observed, whatever the initial kinetic energy. The Ar matrix (or the finite Ar cluster) then undergoes strong perturbations and ejects one or more atoms to create a vacancy for the  $\text{Na}^+$  inclusion. As a first exploratory example, we have also studied the deposition of a neutral  $\text{Na}_6$  cluster. As for the neutral atom, we see also a binding to the surface and no penetration into the Ar substrate. Somewhat surprisingly, there is only little perturbation of the Na cluster internal structure. Continued systematic

investigations on metal cluster deposition in Ar substrate are in progress.

**Acknowledgments:** This work was supported by the DFG, project nr. RE 322/10-1, the French-German exchange program PROCOPE nr. 07523TE, the CNRS Programme “Matériaux” (CPR-ISMIR), Institut Universitaire de France, the Humboldt foundation and a Gay-Lussac price, and has benefited from the CALMIP (CALcul en MIDI-Pyrénées) computational facilities.

### Appendix A. The Na-Ar energy functional in detail

The degrees of freedom of the model are:

- $\{\varphi_n(\mathbf{r}), n = 1 \dots N_{el}\}$  wavefunctions of cluster electrons
- $\{\mathbf{R}_I, I = 1 \dots N_{ion}\}$  coordinates of cluster's  $\text{Na}^+$  ions
- $\{\mathbf{R}_a, a = 1 \dots N_{Ar}\}$  coordinates of Ar atoms (cores  $\text{Ar}^{Q+}$ )
- $\{\mathbf{R}'_a, a = 1 \dots N_{Ar}\}$  coordinates of the Ar valence clouds

An Ar atom is described by two constituents with opposite charge, positive Ar core and negative Ar valence cloud, which allows a correct description of polarization dynamics. We associate a Gaussian charge distribution to both constituents having a width of the order of the 3p shell in Ar, in the spirit of.<sup>32</sup> The dynamical polarizability of the  $\text{Na}^+$  ions is neglected and we treat them simply as charged point particles.

The total energy of the system is composed as:

$$E_{\text{total}} = E_{\text{Nacluster}} + E_{\text{Ar}} + E_{\text{coupl}} + E_{\text{VdW}} \quad ,$$

The energy of the Na cluster  $E_{\text{Nacluster}}$  consists out of TDLDA (with SIC) for the electrons, MD for ions, and a coupling of both by soft, local pseudo-potentials,

see<sup>27,28</sup> for details. The Ar system and its coupling to the clusters is described by

$$\begin{aligned}
E_{\text{Ar}} &= \sum_a \frac{\mathbf{P}_a^2}{2M_{\text{Ar}}} + \sum_a \frac{\mathbf{P}'_a{}^2}{2m_{\text{Ar}}} + \frac{1}{2}k_{\text{Ar}}(\mathbf{R}'_a - \mathbf{R}_a)^2 \\
&\quad + \sum_{a < a'} \left[ \int d\mathbf{r} \rho_{\text{Ar},a}(\mathbf{r}) V_{\text{Ar},a'}^{(\text{pol})}(\mathbf{r}) + V_{\text{ArAr}}^{(\text{core})}(\mathbf{R}_a - \mathbf{R}_{a'}) \right] , \\
E_{\text{coupl}} &= \sum_{I,a} \left[ V_{\text{Ar},a}^{(\text{pol})}(\mathbf{R}_I) + V'_{\text{NaAr}}(\mathbf{R}_I - \mathbf{R}_a) \right] \\
&\quad + \int d\mathbf{r} \rho_{\text{el}}(\mathbf{r}) \sum_a \left[ V_{\text{Ar},a}^{(\text{pol})}(\mathbf{r}) + W_{\text{elAr}}(|\mathbf{r} - \mathbf{R}_a|) \right] , \\
V_{\text{Ar},a}^{(\text{pol})}(\mathbf{r}) &= e^2 q_{\text{Ar}} \left[ \frac{\text{erf}(|\mathbf{r} - \mathbf{R}_a|/\sigma_{\text{Ar}})}{|\mathbf{r} - \mathbf{R}_a|} - \frac{\text{erf}(|\mathbf{r} - \mathbf{R}'_a|/\sigma_{\text{Ar}})}{|\mathbf{r} - \mathbf{R}'_a|} \right] , \\
W_{\text{elAr}}(r) &= e^2 \frac{A_{\text{el}}}{1 + e^{\beta_{\text{el}}(r-r_{\text{el}})}} \\
V_{\text{ArAr}}^{(\text{core})}(R) &= e^2 A_{\text{Ar}} \left[ \left( \frac{R_{\text{Ar}}}{R} \right)^{12} - \left( \frac{R_{\text{Ar}}}{R} \right)^6 \right] \\
V'_{\text{ArNa}}(R) &= e^2 \left[ A_{\text{Na}} \frac{e^{-\beta_{\text{Na}}R}}{R} - \frac{2}{1 + e^{\alpha_{\text{Na}}/R}} \left( \frac{C_{\text{Na},6}}{R^6} + \frac{C_{\text{Na},8}}{R^8} \right) \right] \\
4\pi\rho_{\text{Ar},a} &= \Delta V_{\text{Ar},a}^{(\text{pol})} \\
E_{\text{vdW}} &= e^2 \frac{1}{2} \sum_a \alpha_a \left[ \frac{(\int d\mathbf{r} \mathbf{f}_a(\mathbf{r}) \rho_{\text{el}}(\mathbf{r}))^2}{N_{\text{el}}} - \int d\mathbf{r} \mathbf{f}_a(\mathbf{r})^2 \rho_{\text{el}}(\mathbf{r}) \right] , \\
\mathbf{f}_a(\mathbf{r}) &= \nabla \frac{\text{erf}(|\mathbf{r} - \mathbf{R}_a|/\sigma_{\text{Ar}})}{|\mathbf{r} - \mathbf{R}_a|} . \\
\text{erf}(r) &= \frac{2}{\sqrt{\pi}} \int_0^r dx e^{-x^2} .
\end{aligned}$$

The various contributions are calibrated from independent sources, with a final fine tuning to the NaAr dimer modifying only the term  $W_{\text{elAr}}$ . The parameters are summarized in the table. The third column of the table indicates the source for the parameters.

The (most important) polarization potentials are described by a valence electron cloud oscillating against the raregas core ion. Its parameters are:  $q_{\text{Ar}}$  the effective charge of valence cloud,  $m_{\text{Ar}} = q_{\text{Ar}} m_{\text{el}}$  the effective mass of valence cloud,  $k_{\text{Ar}}$  the restoring force for dipoles, and  $\sigma_{\text{Ar}}$  the width of the core and valence clouds. The  $q_{\text{Ar}}$  and  $k_{\text{Ar}}$  are adjusted to reproduce the dynamical polarizability  $\alpha_D(\omega)$  of the Ar atom at low frequencies, namely the static limit  $\alpha_D(\omega=0)$  and the second derivative of  $\alpha_D''(\omega''=0)$ . The width  $\sigma_{\text{Ar}}$  is determined consistently such that the restoring force from the folded Coulomb force (for small displacements) reproduces the spring constant  $k_{\text{Ar}}$ .

$V_{\text{Ar},a}^{(\text{pol})}$	$q_{\text{Ar}} = \frac{\alpha_{\text{Ar}} m_{\text{el}} \omega_0^2}{e^2}$ , $k_{\text{Ar}} = \frac{e^2 q_{\text{Ar}}^2}{\alpha_{\text{Ar}}}$ , $m_{\text{Ar}} = q_{\text{Ar}} m_{\text{el}}$ $\sigma_{\text{RG}} = \left( \alpha_{\text{Ar}} \frac{4\pi}{3(2\pi)^{3/2}} \right)^{1/3}$	$\alpha_{\text{Ar}} = 11.08 \text{ a}_0^3$ $\omega_0 = 1.755 \text{ Ry}$
$W_{\text{elAr}}$	$A_{\text{el}} = 0.47$ , $\beta_{\text{el}} = 1.6941 / \text{a}_0$ , $r_{\text{el}} = 2.2 \text{ a}_0$	fit to NaAr
$V_{\text{ArAr}}^{(\text{core})}$	$A_{\text{Ar}} = 1.367 * 10^{-3} \text{ Ry}$ , $R_{\text{Ar}} = 6.501 \text{ a}_0$	fit to bulk Ar
$V'_{\text{ArNa}}$	$\beta_{\text{Na}} = 1.7624 \text{ a}_0^{-1}$ , $\alpha_{\text{Na}} = 1.815 \text{ a}_0$ , $A_{\text{Na}} = 334.85$ $C_{\text{Na},6} = 52.5 \text{ a}_0^6$ , $C_{\text{Na},8} = 1383 \text{ a}_0^8$	after <sup>31</sup>

The short range repulsion is provided by the various core potentials. For the Ar-Ar core interaction we employ a Lennard-Jones type potential with parameters reproducing binding properties of bulk Ar. The Na-Ar core potential is chosen according to,<sup>31</sup> within properly avoiding double counting of the the dipole polarization-potential.

The pseudo-potential  $W_{\text{elAr}}$  for the electron-Ar core repulsion has been modeled according to the proposal of<sup>32</sup> with a final slight adjustment to the Na-Ar dimer, data taken from from<sup>36</sup> and.<sup>37</sup>

The Van-der-Waals energy  $E_{\text{VdW}}$  is a correlation from the dipole excitation in the Ar atom coupled with a dipole excitation in the cluster. We exploit that  $\omega_{\text{Mie}} \ll \Delta E_{\text{Ar}}$  which simplifies the term to the variance of the dipole operator in the cluster, using again the regularized dipole operator  $\mathbf{f}_a$  corresponding to the smoothened Ar charge distributions. The full dipole variance is simplified in terms of the local variance.

## References

1. H. Brune, in “Metal Clusters at Surfaces, Structures”, eds. K. H. Meiwes-Broer, Springer, Berlin, 2000.
2. Proceedings of ISSPIC9, Lausanne 1998, Eur. Phys. J. **D9** (1999)
3. Proceedings of ISSPIC10, Atlanta 2000, Eur. Phys. J. **D16** (2001)
4. Proceedings of ISSPIC11, Strasbourg 2002, Eur. Phys. J. **D24** (2003)
5. Proceedings of ISSPIC12, Nanjing 2004, Eur. Phys. J. **D34** (2005)
6. C. Binns, Surf. Sci. Rep. **44**, 1 (2001).
7. W. Harbich, in “Metal Clusters at Surfaces, Structures”, eds. K. H. Meiwes-Broer, Springer, Berlin, 2000
8. Y. Z. Li, R. Reifengerger, R. P. Andres, Surf. Sci. **250**, 1 (1991)
9. D. M. Schaefer, A. Patil, R. P. Andres, R. Reifengerger, Phys. Rev. **B51**, 5322 (1995)
10. Ch. Kuhrt, M. Harsdorff, Surf. Sci. **245**, 252 (1995)
11. R. N. Barnett, U. Landman, Phys. Rev. Lett **67**, 727 (1991)
12. H. P. Cheng, U. Landmann, Science **260**, 1304 (1991)
13. H. Häkkinen, R. N. Barnett, U. Landmann, Eur. Phys. Lett. **28**, 263 (1994)
14. H. Häkkinen, M. Manninen, Eur. Phys. Lett. **34**, 177 (1996)
15. C. Kohl, P.-G. Reinhard, Z. Phys. D **38**, 81 (1996)

16. C. Kohl, P.-G. Reinhard, Z. Phys. D **39**, 225 (1997)
17. C. Kohl, E. Suraud, P.-G. Reinhard, Eur. Phys. J. **D11** 115 (2000)
18. A. Ipatov, E. Suraud, P.-G. Reinhard, Int. J. Mol. Sci. **4**, 301 (2003)
19. A. Ipatov, P.-G. Reinhard and E. Suraud, Eur. Phys. J **D30**, 65 (2004).
20. B. Gervais, E. Giglio, E. Jacquet, A. Ipatov, P.-G. Reinhard, and E. Suraud, J. Chem. Phys. **121**, 8466 (2004)
21. F. Fehrer, M. Mundt, P.-G. Reinhard, and E. Suraud, Ann. Phys. (Leipzig) **14**, 411 (2005)
22. F. Fehrer, P.-G. Reinhard and E. Suraud, Appl. Phys. **A82**, 145 (2005)
23. M. J Field, P. A. Bash, and M. Karplus, J. Comp. Chem. **11**, 700 (1990)
24. J. Gao, Acc. Chem. Res. **29**, 298 (1996)
25. N. Gresh and D. R. Garmer, J. Comp. Chem. **17**, 1481 (1996)
26. F. Fehrer, P.-G. Reinhard, E. Suraud, E. Giglio, B. Gervais, and A. Ipatov, Appl. Phys. **A82**, 151 (2005)
27. P.-G. Reinhard and E. Suraud, *Introduction to Cluster Dynamics*, Wiley, New York, 2003
28. F. Calvayrac, P.-G. Reinhard, E. Suraud, and C. A. Ullrich, Phys. Rept. **337**, 493 (2000)
29. S. Kuemmel, P.-G. Reinhard, and M. Brack, Euro. Phys. J. **D9**, 149 (1999)
30. B. G. Dick and A. W. Overhauser, Phys. Rev. **112**, 90 (1958)
31. G. Reza Ahmadi, J. Almlöf, and J. Roegen, *Chem. Phys.* **199**, 33 (1995)
32. F. Dupl e and F. Spiegelmann, J. Chem. Phys. **105**, 1492 (1996)
33. B. Montag and P.-G. Reinhard, Z. Phys. D **33**, 265 (1995)
34. B. Montag and P.-G. Reinhard, Phys. Lett. **A193**, 380 (1994)
35. C. Kohl, F. Calvayrac, P.-G. Reinhard, E. Suraud, Surf. Sci **405**, 74 (1998)
36. M. Gross and F. Spiegelmann, J. Chem. Phys. **108**, 4148 (1998)
37. M. B. El Hadj Rhouma, H. Berriche, Z. B. Lakhdar, and F. Spiegelman. J. Chem. Phys., **116**, 1839 (2002)
38. P. M. Dinh, F. Fehrer, P.-G. Reinhard, E. Suraud, and G. Bousquet, in preparation.